research papers

Growth kinetics, diffraction properties and effect of agarose on the stability of a novel crystal form of *Thermus thermophilus* aspartyl-tRNA synthetase-1

Dao-Wei Zhu,[a]† **Bernard Lorber,**[a]* **Claude Sauter,**[a]‡ **Joseph D. Ng,**[a]§ **Philippe Bénas,**[a]¶ **Christian Le Grimellec**[b] **and Richard Giegé**[a]

[a]Département 'Mécanismes et Macromolécules de la Synthèse Protéique', UPR 9002, Institut de Biologie Moléculaire et Cellulaire du CNRS, 15 Rue René Descartes, 67084 Strasbourg, France, and [b]Centre de Biochimie Structurale, INSERM U414, 29 Rue de Navacelles, 34090 Montpellier, France

† Present address: MRC Group in Molecular Endocrinology, CHUL Research Center and Laval University, Quebec G1V 4G2, Canada.
‡ Present address: European Molecular Biology Laboratory, Structural Biology, Postfach 10.2209, 69012 Heidelberg, Germany.
§ Present address: Laboratory for Structural Biology and Department of Biological Sciences, 254 Wilson Hall, University of Alabama, Huntsville, AL 35899, USA.
¶ Present address: Faculté de Pharmacie Paris V, 4 Avenue de l'Observatoire, 75270 Paris CEDEX 06, France.

Correspondence e-mail:
b.lorber@ibmc.u-strasbg.fr

Growth kinetics and diffraction properties of monoclinic crystals of eubacterial *Thermus thermophilus* aspartyl-tRNA synthetase-1 (AspRS-1) prepared in the presence of polyethylene glycol and agarose are studied. Their solubility and two-dimensional phase diagram are compared with those of orthorhombic crystals which grow in the presence of sodium formate or ammonium sulfate. The growth mechanism of the novel crystals was monitored by atomic force microscopy. The gel stabilizes the crystal lattice under the cryogenic conditions used for structure determination at high resolution.

1. Introduction

Crystallogenesis studies on biological macromolecules aim towards understanding nucleation and crystal growth processes and towards finding ways to improve crystal quality. Here, we search for a correlation between crystal growth conditions (*e.g.* the nature of the crystallizing agent, protein supersaturation and crystal growth rate) and crystallographic properties (*e.g.* the habit, space group, diffraction intensity, resolution and mosaicity).

In terms of mechanism, the crystallization of proteins obeys the same rules as inorganic or small organic molecules (McPherson, 1998; Chernov, 1998; Ducruix & Giegé, 1999), except that the former are stable within a limited range of physical chemical conditions (temperature, pH, ionic strength, pressure *etc.*). The solubility of most proteins decreases in the presence of a solute (such as a salt, an alcohol or a polymer), but a high relative supersaturation is often a prerequisite to nucleation. By varying the solute, different crystalline polymorphs may be obtained (Ducruix & Giegé, 1999). Protein crystals prepared within a gel where convection is reduced may have better morphologies and superior diffraction properties (Miller *et al.*, 1992; DeLucas *et al.*, 1994; Lorber, Sauter, Ng *et al.*, 1999; Lorber, Sauter, Robert *et al.*, 1999; Vidal *et al.*, 1998, 1999).

Here, crystals of the thermostable enzyme aspartyl-tRNA synthetase (AspRS-1) from *T. thermophilus* were produced in various media. In addition to a crystal form growing in the presence of salt (Poterszman *et al.*, 1993; Delarue *et al.*, 1994; Ng *et al.*, 1996), a novel form was prepared in the presence of polyethylene glycol (PEG) and agarose. Its solubility was measured and a two-dimensional phase diagram was established. Growth kinetics of individual crystals were plotted and the crystal faces were examined by atomic force microscopy (AFM). Crystals prepared in the gel were more suitable for the collection of X-ray diffraction intensities at high resolution under cryogenic conditions than crystals prepared in solution under otherwise identical conditions. Differences between

crystal forms are discussed with respect to growth mechanism and diffraction properties, and advantages of the gel are emphasized.

2. Materials and methods

2.1. Protein and chemicals

The thermophilic bacterium *T. thermophilus* has two aspartyl-tRNA synthetases (AspRS) which differ in their sequences and catalytic properties. For the present work, AspRS-1 was overproduced in *Escherichia coli* and purified as described by Poterszman *et al.* (1993) and Ng *et al.* (1996). Size-exclusion chromatography on a Sephacryl S-200HR column as a final purification step was essential for the reproducibility of crystallization results. The enzyme was stored at 277 K in 50 mM Tris–HCl buffer adjusted to pH 7.2 and containing 10 mM MgCl$_2$ and 0.5 mM dithiothreitol (DTT). Protein concentration was calculated from the absorbance (E_{280nm} = 1.0 ml mg^{-1} cm^{-1}) and the aminoacylation activity was measured according to the procedure described by Poterszman *et al.* (1993). Ultrapure PEG 8000 (Cat. No. P-4463) was purchased from Sigma and Aristar grade ammonium sulfate from BDH. Other chemicals were of *pro analysi* grade. All solutions were prepared with thrice-distilled water and filtered through 0.2 µm pore-size membranes. Low gelling point [T_g = 301 K at 1%(m/v)] agarose was a gift from So.Bi.Gel (Hendaye, France).

2.2. Crystallization in solution and in gel

Protein samples filtered on 0.2 µm Ultrafree-MC membranes (Cat. No. UFC 30GV00, Millipore) were crystallized by vapour diffusion in hanging drops prepared in Linbro plates. Assays with sodium formate or ammonium sulfate were prepared as described previously (Poterszman *et al.*, 1993; Ng *et al.*, 1996). Crystals were prepared at 293 K in the presence of PEG 8000 using a sparse matrix (Hampton Research, Laguna Niguel, CA) and were improved by varying parameters in 1–5 µl drops equilibrated against 1 ml reservoirs. Assays with gel were prepared by mixing appropriate volumes of 2%(m/v) agarose stock solution (heated to 363 K) and crystallizing agent solution (at 293 K) in a small tube. Protein solution (at 293 K) was added once the solution had cooled to 308 K and aliquots of the mixture were immediately dispensed onto siliconized glass coverslips before sealing over reservoirs.

2.3. Growth kinetics and solubility measurements

Crystals were measured on video images taken at regular time intervals with an optical microscope (Labophot, Nikon) equipped with a colour CCD camera (IRIS, Sony). Incubators set to 277, 283, 288, 293 or 303 K were used to control temperature. After an equilibration period of 50 d, the residual protein concentration in equilibrium with crystals (or solubility s) was titrated on 5 µl centrifuged mother liquor using a dye-binding assay (Bradford, 1976; Mikol *et al.*, 1990). When c is the protein concentration in the drop before crystallization, the supersaturation is given by $\Delta c = c - s$, the

excess of supersaturation by $\beta = c/s$ and the relative supersaturation by $\sigma = \beta - 1 = (c - s)/s$ (Boistelle & Astier, 1988). When Δc is low, σ can be approximated by $\ln(c/s)$.

2.4. Atomic force microscopy imaging

AFM was performed in tapping mode using a Nanoscope III Multimode system (Digital Instruments, Santa Barbara, CA, USA). Crystals were grown at 293 K by vapour diffusion in 5 µl drops containing 8%(m/v) PEG 8000 and 0.1 M Tris–HCl pH 8.5 deposited on acid-treated glass cover slips. The latter were glued to magnetic punches and mounted in a fluid cell without an O ring (Le Grimellec *et al.*, 1998). Throughout all steps, crystals were kept in solution and the PEG concentration was increased by 1%(m/v) to compensate for temperature change to 298 K in the fluid cell (under these conditions, crystals neither dissolved nor grew). V-shaped sharpened silicon nitride cantilevers (tip-end angle 18° over 200 nm, nominal spring constant 0.1 N m^{-1}; Park Scientific, Sunnyvale, CA, USA) were used for imaging (J scanner). In most experiments, driving frequency was between 7.9 and 9.3 kHz (experiments using a frequency ~32 kHz gave similar results). Set point was kept 5–10% below the free cantilever amplitude. Scan rates varied between 0.4 and 3.8 Hz according to scan sizes.

2.5. Preliminary crystallographic analysis

The orientation of crystal axes relative to faces was determined using a sample holder designed for mosaicity measurements (Lorber, Sauter, Ng *et al.*, 1999). Crystals were characterized at 293 K with Ni-filtered Cu $K\alpha$ radiation (λ = 1.54 Å) on a Nonius rotating-anode generator coupled to a MacScience DIP 2000b IP detector. A 3.1 Å resolution data set was collected at room temperature from a form B crystal prepared in solution (completeness 84%; R_{sym} 6.4%) (Otwinowsky & Minor, 1997). Monoclinic space group $P2_1$ was assigned on the basis of the Laue symmetry in conjunction with systematic extinctions. Molecular replacement using the orthorhombic AspRS structure (Delarue *et al.*, 1994; Poterszman *et al.*, 1994) as a search model with the software *AMoRe* (Navaza & Saludjian, 1997) gave an unambiguous solution in $P2_1$ (correlation 67.3%; R factor 32.7%). On the beamline BW7B (DESY, Hamburg) a complete data set at 2.65 Å was collected from a flash-cooled crystal grown in gel and soaked for 10 s in a mother liquor containing 30%(v/v) glycerol.

3. Results

3.1. A second crystal form for thermostable AspRS-1

Two crystal forms of AspRS-1 have been prepared from the same protein batch by varying the nature of the crystallizing agent. Orthorhombic crystals (form A) obtained in the presence of either sodium formate or ammonium sulfate are used as a reference (Table 1). In agarose gel, crystals grow from precipitate within 48–72 h and measure 0.4 × 0.2 × 0.2 mm after six months. A second crystal form (form B),

Table 1
Crystallization and preliminary crystallographic data of AspRS crystal forms.

All crystals were prepared with a single protein batch. The diffraction limit is defined such as 80% of the reflections have intensities with $I/\sigma(I) \geq 3$.

	Form A	Form B
Crystallization		
Medium	Solution or 0.1%(m/v) agarose gel	Solution or 0.1%(m/v) agarose gel
Temperature range (K)	277–293	277–293
Precipitant	4 M Na formate or 2 M NH$_4$ sulfate	4–8%(m/v) PEG 8000
Protein concentration (mg ml^{-1})	16	16
Buffer	50 mM Tris–HCl	100 mM Tris–HCl
pH	7.2	7.8
Additives	10 mM MgCl$_2$, 0.5 mM DTT	10 mM MgCl$_2$, 0.5 mM DTT
Time (at 293 K)	2–3 d	≤2 h (2–3 d in gel)
Largest crystal size (mm)	0.4 × 0.2 × 0.2	0.8 × 0.8 × 0.2
X-ray data collection at 293 K		
Space group	$P2_12_12_1$	$P2_1$
Unit-cell parameters (Å,°) and volume (Å^3)	$a = 61.0$, $b = 156.1$, $c = 177.3$, $V = 1.7 \times 10^6$	$a = 85.1$, $b = 113.3$, $c = 90.2$, $\beta = 104.3$, $V = 0.84 \times 10^6$
Diffraction limit (Å)	2.0	2.65
$I/\sigma(I)$ overall	15.2	20.0
$I/\sigma(I)$ in the last shell	3.1 (2.05–2.00 Å)	8.1 (2.74–2.65 Å)
Reference	Ng et al. (in preparation)	This paper

found with a sparse matrix, grows as thin plates in the presence of PEG. Electrophoresis indicates that it contains a polypeptide chain (apparent M_r of 66 000) identical to that of the initial protein. After a refinement of the crystallization condition (by varying protein, PEG and agarose concentrations as well as temperature and pH; see Fig. 1), monoclinic crystals with a well developed morphology and a greater volume (0.8 × 0.8 × 0.2 mm) can be produced within two weeks at 293 K. Table 1 compares the diffraction characteristics of both crystal forms. The diffraction limit of the orthorhombic crystals is 2.0 Å and a complete diffraction data set was collected at 293 K on a synchrotron beamline (Ng et al., in preparation). For monoclinic crystals prepared in solution, a first complete data set at 3.1 Å resolution was collected at room temperature on a rotating-anode generator. At 293 K, their diffraction limit is actually 2.6 Å on a synchrotron beamline, but they are unstable and freezing is not satisfactory for data collection under cryogenic conditions. The same crystals prepared in agarose have similar diffraction properties but can be frozen; they are suitable for data collection at 2.65 Å resolution.

3.2. Phase diagram of AspRS-1

In Fig. 2, the solubility of AspRS in the absence of agarose at 293 K decreases from 3.3 to 0.3 mg ml^{-1} when the PEG concentration increases from 2 to 10%(m/v). The excess of protein supersaturation (β) ranges from 1 to 80 in the two-dimensional diagram. Inset images display the crystal habits under various experimental conditions. The best morphology is obtained in the part of the nucleation zone where $\beta = 15$–20. As soon as $\beta > 21$ a precipitate forms at either high protein or PEG concentration in solution and in gel.

3.3. Growth kinetics of form B

Fig. 3(a) displays images of a monoclinic crystal growing in PEG solution. Growth is preceded by a lag time whose duration ranges from <1 h to >10 d at 303 and 277 K, respectively (Fig. 3b and Table 2). The latter strongly depends upon protein concentration, being 20 times shorter when it is raised from 15 to 30 mg ml^{-1} (Fig. 3c). The highest growth rate (~70 μm h^{-1} at 303 K; Table 2) decreases by a factor of 60 when the temperature is lowered by 26 K. Rates in solution and in 0.1%(m/v) agarose gel are similar.
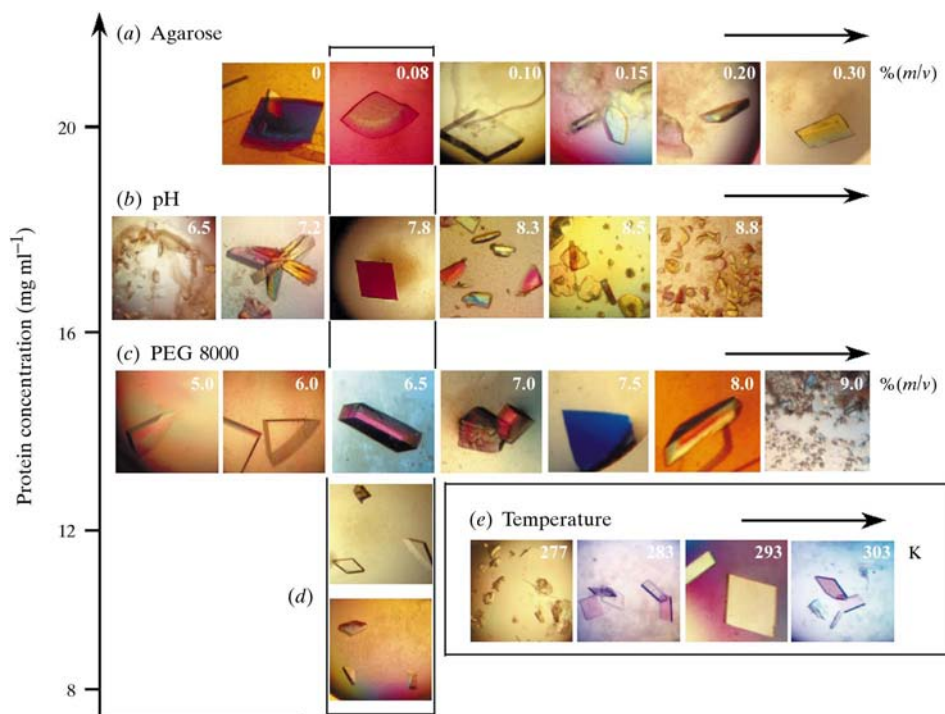

Figure 1
Effect of five variables on the crystallization of form B crystals of AspRS. Variables are: (a) agarose concentration [at 6.5%(m/v) PEG, 20 mg ml^{-1} protein, pH 7.8 and 293 K], (b) pH [at 6.5%(m/v) PEG, 0.1%(m/v) agarose, 16 mg ml^{-1} protein and 293 K], (c) PEG 8000 concentration [at 0.1%(m/v) agarose, 16 mg ml^{-1} protein, pH 7.8 and 293 K], (d) protein concentration at 293 K in the presence of 0.1%(m/v) agarose at pH 7.8 (vertical axis and boxed images) and (e) temperature [at 6.5%(m/v) PEG, 0.1%(m/v) agarose, 16 mg ml^{-1} protein and pH 7.8]. All views at the same scale show only a part of the crystallization drop. The largest crystal is 0.6 mm long.

Table 2
Lag time, crystal size and growth rate of form *B* crystals in solution.

Experimental conditions are as in Fig. 3. Supersaturation excess is ~25.

Temperature (K)	Lag time† (h)	Final crystal length (µm)	Highest growth rate		
			(μm h^{-1})	(Å s^{-1})	(s molecule^{-1})
277	264 ± 5	180 ± 20	1.1 ± 0.2	3.1 ± 0.6	31 ± 6
293	2.0 ± 0.2	350 ± 20	39 ± 3	108 ± 11	0.9 ± 0.1
303	0.7 ± 0.1	400 ± 20	68 ± 10	189 ± 28	0.5 ± 0.1

† Lag time was 108 ± 12 and 9 ± 3 h at 283 and 288 K, respectively.

3.4. AFM analysis of crystal surface

The surface of form *B* crystals prepared in solution under conditions within the region of the phase diagram highlighted in yellow (see Fig. 2) was examined by AFM. Images of (100) lozenge-shaped faces (Fig. 4a), measuring 150–200 µm on the edge, consistently show one major asymmetrically elongated hillock, sometimes overgrown by a few secondary ones (Fig. 4b). Eight out of ten crystals that have ceased to grow after 2–12 h exhibit a single dislocation source with a screw component perpendicular to the surface. The latter generates a clockwise-rotating and sometimes quasi-circular spiral with over 100 turns and a radius ≥80 µm. The terraces with a height of 8.0 ± 0.1 nm (standard deviation on 28 measurements) are formed by a single layer of protein molecules. High-resolution scans reveal alignments of individual synthetase molecules with an average diameter of 10 nm, in agreement with the packing calculated from X-ray diffraction data (Fig. 4c). Scans of the other crystal faces do not reveal any ordered pattern (not shown).

4. Discussion

4.1. The benefit of growing crystals in gel

Monoclinic AspRS crystals prepared in PEG solution are more sensitive to temperature fluctuation and to radiation damage at 293 K than orthorhombic crystals prepared in salt solution. Temperature, protein concentration and pH have essentially the same effects when crystals grow in solution or in dilute agarose gel, but in the latter medium microcrystals remain stationary at the place where they nucleate and their morphology can develop beautifully in three dimensions with minimal defects. The full-width at half-maximum of Bragg reflections of these crystals is smaller (11 arcsec) than that of those prepared in salt solution (14–27 arcsec) (Lorber, Sauter, Ng *et al.*, 1999). This may be a consequence of the reduction of thermal and density-driven or surface tension-driven convection which causes uncontrolled turbulence in solution and disturbs the regular assembly of macromolecules. In the case of thaumatin crystals, the gel was proposed to mimic in part the effects of weightlessness (Lorber, Sauter, Robert *et al.*, 1999). This non-convective environment is comparable to that existing in capillary tubes. In the gel-acupuncture technique, diffusion is controlled to grow centimetre-long single protein crystals (Garcia-Ruiz & Moreno, 1997; Moreno & Soriano-

Garcia, 1999). Here, the benefit of agarose gel is that the crystals can be used for data collection under cryogenic conditions, perhaps because carbohydrate chains occupy the solvent channels. Finally, twinning was eliminated in monoclinic crystals of *Sulfolobus solfataricus* alcohol dehydrogenase by growing them in a gel (Sica *et al.*, 1994).

4.2. Solubility of AspRS in PEG *versus* salt solution

In aqueous solution, neutral inorganic salts either stabilize or destabilize protein molecules when they are either excluded (with regard to water) from their surface or in interaction with their unfolded backbone (Timasheff & Arakawa, 1988). After the empirical work of Hofmeister, ions are ranked according to their effectiveness in solubilizing proteins (see, for example, Riès-Kautt & Ducruix, 1989). Repulsion or attraction depends upon the salt's ability to screen the electrostatic charges of the macromolecule and upon the net charge of the latter. For acidic proteins, ions follow Hofmeister's series (Cacace *et al.*,
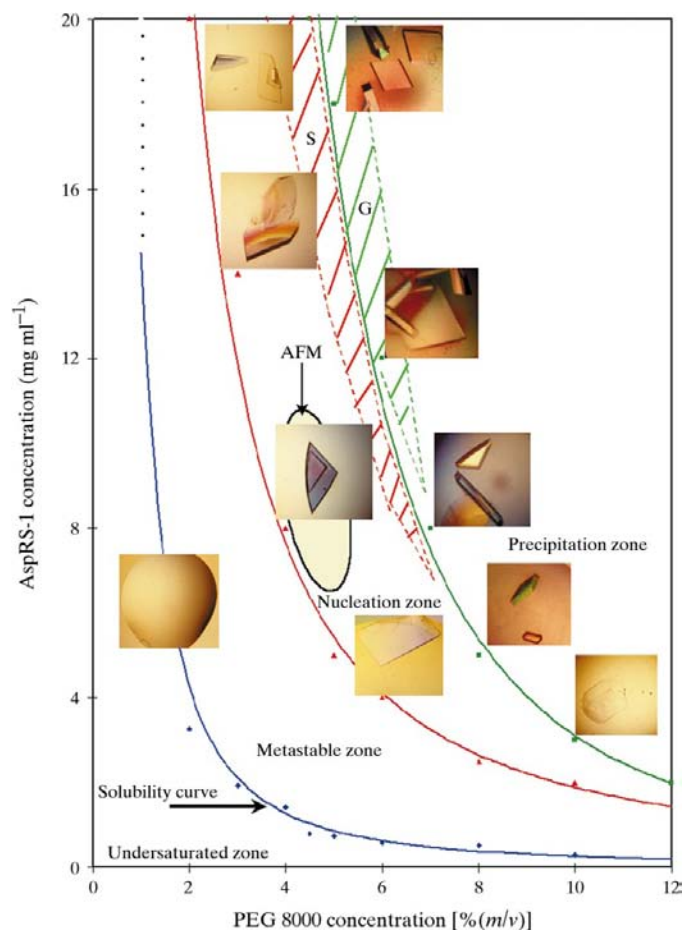
Figure 2
Two-dimensional phase diagram of form *B* crystals of AspRS at 293 K. Diamonds indicate protein solubility at *t* = 50 d. Triangles and squares, respectively, demarcate nucleation and precipitation zones determined by visual examination at 50-fold magnification. Lines are only a guide for the eye. Each image is placed at the corresponding experimental condition. S and G, red and green hatched regions where the best crystals grow in solution and in gel, respectively; AFM, region (in yellow) in which crystals are taken for AFM studies.

1997); for basic proteins, the order is reversed (Riès-Kautt & Ducruix, 1989). Beyond the salting-in region, solubility s can be approximated by the linear function

$$\log s = b - K_s C_s,$$

where C_s is the salt concentration, K_s is the slope and b is the intercept extrapolated at $C_s = 0$. For orthorhombic AspRS crystals in ammonium sulfate (Ng *et al.*, 1996), $b = 1.5$ and $K_s = -0.98$ at 277 K (-0.48 at 293 K) (Fig. 5a). At high supersaturation, their growth is concomitant with the dissolution of a precipitate (Ng *et al.*, 1996; Zhu *et al.*, 1999), as observed for other proteins (see, for example, Boistelle & Astier, 1988),

Polyethylene glycols (PEGs) with the general formula $H(OCH_2CH_2)_nOH$ are neutral water-soluble polyol chains known for their effectiveness in salting out proteins (McPherson, 1976; Atha & Ingham, 1981). In aqueous solution, they act on proteins *via* a mechanism that is similar to that of salts. When they are excluded from protein's surface, the latter is preferentially hydrated and soluble; when there is competition for water the protein becomes insoluble and aggregates (Timasheff & Arakawa, 1988). The effect depends in part upon the hydrophobicity of the protein (Lee & Lee, 1981). Denaturation results from an imbalance between preferential interactions with the folded native and the unfolded polypeptide chain. Protein crystallization from PEG solutions may be consecutive to a phase separation (Alber *et al.*, 1981; McPherson, 1976). For AspRS, there is a linear relationship between solubility and PEG 8000 concentration

(Fig. 5b). In the presence of PEG or salt, AspRS crystallizes either readily from solution or only after precipitation.

The combination of the solubility data of AspRS in the presence of ammonium sulfate or PEG gives a linear plot (Fig. 5c) that can be fitted with the relation

$$C_{\text{ammonium sulfate}} = 0.87 C_{\text{PEG 8000 [\%(m/v)]}},$$

where C is the concentration of the solute (*i.e.* the crystallizing agent). Hence, under otherwise identical conditions, an increment of $1\%(m/v)$ PEG 8000 has the same effect on AspRS solubility as $1.15\ M$ ammonium sulfate and PEG is 920 times more effective than the salt on a molar basis (15 times on a mass basis). It follows that a $0.87\ M$ ammonium sulfate solution is equivalent to a $40\%(m/v)$ PEG 8000 solution with regard to vapour pressure and that the effect of PEG is 23 times stronger than that of the salt on a molar basis (Arakali *et al.*, 1995).

4.3. Kinetic aspects of crystal growth

Graphs of crystal length *versus* growth time in solution (Fig. 2b) can be fitted with the equation

$$L_{\max} - L = \{1 - \exp[-(t - t_0)/\tau]\},$$

where L and $L_{\max}$ are current and maximal crystal lengths, t is time, t_0 is the lag time and τ is a time constant. The lag time (derived by extrapolation to zero length) ranges from <1 to ~11 d (264 h) when temperature decreases from 303 to 277 K (Table 2). It decreases from 1.5 h to 8 min when protein concentration rises from 15 to 25 mg ml^{-1} (Fig. 2c). Control experiments set up at 293 K with a solution containing $7\%(m/v)$ PEG 8000, 100 mM Tris–HCl buffer and 15 mg ml^{-1} bovine serum albumin indicate that 5 µl drops take 10 d to reach 95% of equilibration at 293 K (result not shown). In experiments with AspRS at the same temperature, the lag time represents only 1/120 of the time required to transfer 5 µl water towards the reservoir. Consequently, the synthetase crystals nucleate and start to grow before drop equilibration is completed. The lag time is likely to correspond to the time required to reach the excess of supersaturation and to trigger nucleation.
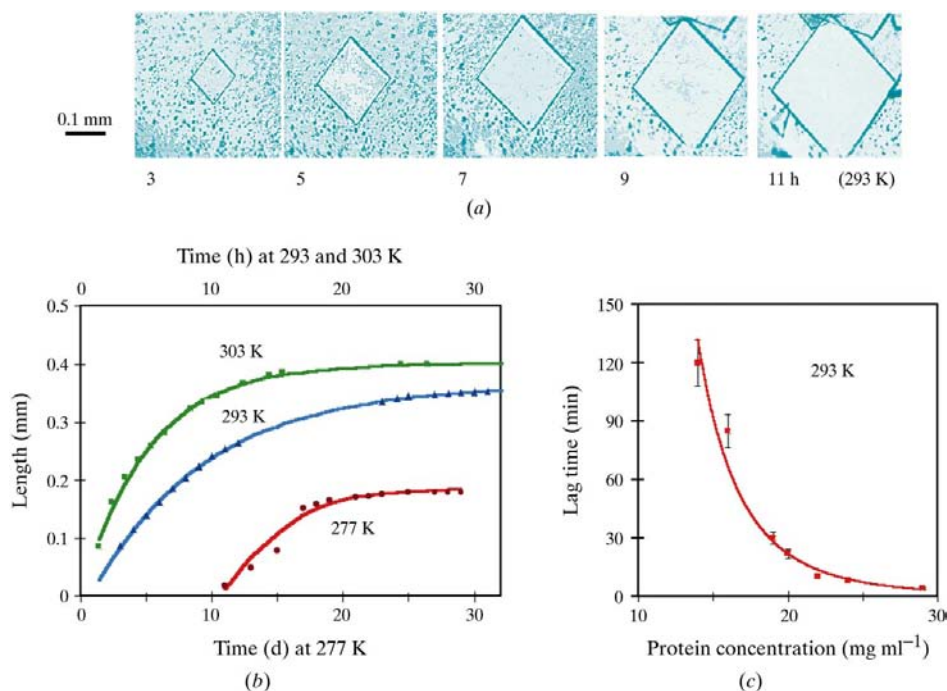
The growth rate of form B crystals increases quasi-linearly by 2.5 µm h^{-1} K^{-1} from 1.1 to 68 µm h^{-1} when the temperature is raised from 277 to 303 K (Table 2). For crystals of similar final size, the rate is 4.2 µm h^{-1} (in 0.8 M ammonium sulfate at 293 K) and only

Figure 3
Effect of temperature and protein concentration on growth of form B crystals of AspRS. (a) Growth of a plate-like crystal at 293 K. (b) Growth kinetics at 277, 293 and 303 K. Respective lag times are 0.7 h, 1 h and 10 d. (c) Variation of lag time with protein concentration at 293 K. Hanging drops containing 14 mg ml^{-1} enzyme, $6.5\%(m/v)$ PEG 8000, 0.5 mM DTT and 100 mM Tris–HCl adjusted to pH 7.8 were kept at 293 K. Kinetics are similar in the presence of $0.1\%(m/v)$ agarose.

$0.32 \ \mu m \ h^{-1}$ (at 277 K) when growth is limited by the dissolution rate of a precipitate (Ng *et al.*, 1996).

4.4. Peculiar features of the growth in agarose gel

In solution, the best crystals of form *A* grow with a rate of $4.2 \ \mu m \ h^{-1}$ at $\beta = c/s$ as low as 1.9 (at 293 K and 20 mg ml^{-1} protein in $0.8 \ M$ ammonium sulfate; Ng *et al.*, 1996). This contrasts with form *B* crystals, which grow larger at a tenfold higher rate and at a tenfold higher β (in the region marked S and hatched in red in Fig. 3). In agarose, the largest form *B* crystals grow on the right side of the precipitation curve in a region where $\beta = 21$–25 (marked G and hatched in green in Fig. 2). Consequently, a greater driving force is required in the gel, where crystals do not sediment to the bottom of the solution. This is apparently in contradiction to the observation made on lysozyme that agarose promotes nucleation (Robert *et al.*, 1994; Vidal *et al.*, 1998).

4.5. Growth mechanism monitored by AFM

In situ AFM images of the surface of AspRS crystals grown at $\beta = 7$–10 and at a rate $>50 \ \mu m \ h^{-1}$ show neither two-dimensional (islands) nor three-dimensional nucleation (Fig. 4). Only one or a few spiral patterns are observed, indicating that growth proceeds exclusively by a screw dislocation mechanism, as is known from crystals of small molecules and other biological particles at low supersaturation (*e.g.* Liu *et al.*, 1995; Kuznetsov *et al.*, 1996; Ng *et al.*, 1997; Sangwal, 1998; Malkin *et al.*, 1999). Alignments of regularly spaced steps parallel to the crystal edges are observed far from the dominant spiral centre (Fig. 4). Assuming a constant growth rate, the average angular velocity of the terraces is $\sim 0.02 \ rad \ s^{-1}$ on the (100) face. Their average step height of 8 nm along the *a* axis corresponds to one layer of synthetase dimers. The resulting slope of the polyhedral hillock covering the entire crystal face (from the top of the spiral to its edge) is thus 1–2%. The arrangement of individual particles (seen on high-resolution scans) which have an average diameter of 10 nm superposes well with that deduced from molecular packing (top right panel in Fig. 4) (Charron *et al.*, 2001). The AFM images also show lattice defects such as a misalignment of AspRS molecules similar to those described previously for other macromolecules (Malkin *et al.*, 1996).
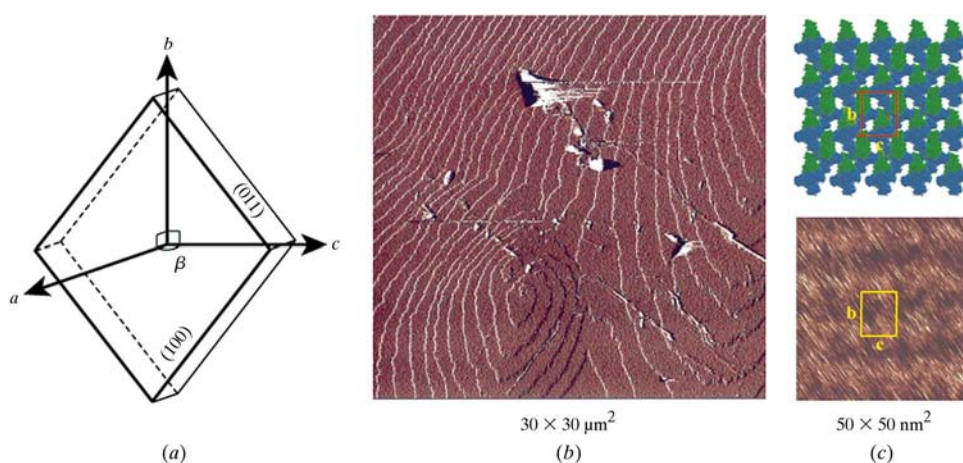

Figure 4
In situ AFM of freshly grown form *B* AspRS crystals. (*a*) Crystal morphology; (*b*) scan of a 30 × 30 mm surface area of the (100) face of a 100 × 100 mm lozenge-shaped tabular crystal seen down the *a* axis. White marks result from scratches or debris attached to the cantilever or to the crystal surface; (*c*, bottom panel) scan of a 50 × 50 nm area of the surface of the (100) face; (*c*, top panel) two-dimensional array of synthetase molecules determined from crystallography data (Charron *et al.*, 2001). The unit cell and *b* and *c* axes are indicated.
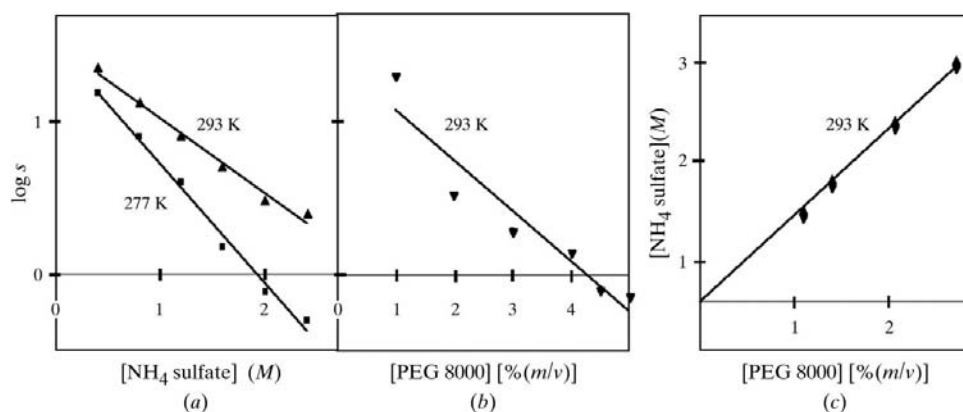
Figure 5
Comparative solubility of AspRS in ammonium sulfate *versus* PEG 8000. (*a*, *b*) Plot of log of solubility at 293 K *versus* (*a*) salt molarity (linear regressions give log $s = -0.98 \ M \pm 1.6$ at 277 K and log $s = -0.48 \ M \pm 1.5$ at 293 K) and (*b*) PEG 8000 concentration [log $s = -0.33\%(m/v) \pm 1.4$]. (*c*) Equivalence between log s in the presence of ammonium sulfate and log s in the presence of PEG 8000 (at 293 K). Experimental points can be fitted by the linear equation $C_{ammonium \ sulfate} = 0.87 \ C_{PEG \ 8000}$, where C stands for concentration. Symbol size indicates experimental error. Data for ammonium sulfate are taken from Ng *et al.* (1996).

research papers

References

Alber, T., Hartman, F. C., Johnson, R. M., Petsko, G. A. & Tsernoglou, D. (1981). *J. Biol. Chem.* **256**, 1356–1361.

Arakali, S. V., Luft, J. R. & DeTitta, G. T. (1995). *Acta Cryst.* D**51**, 772–779.

Atha, D. H. & Ingham, K. C. (1981). *J. Biol. Chem.* **256**, 12108–12117.

Boistelle, R. & Astier, J. P. (1988). *J. Cryst. Growth*, **90**, 14–30.

Bradford, M. (1976). *Anal. Biochem.* **72**, 248–254.

Cacace, M. G., Landau, E. M. & Ramsden, J. J. (1997). *Quart. Rev. Biophys.* **30**, 241–277.

Charron, C., Sauter, C., Zhu, D. W., Ng, J. D., Kern, D., Lorber, B. & Giegé, R. (2001). In the press.

Chernov, A. A. (1998). *Acta Cryst.* A**54**, 859–572.

Delarue, M., Poterszman, A., Nikonov, S., Garber, M., Moras, D. & Thierry, J. C. (1994). *EMBO J.* **13**, 3219–3229.

DeLucas, L. J., Long, M. M., Moore, K. M., Rosenblum, W. M., Bray, T. L., Smith, C., Carson, M., Narayana, S. V. L., Carter, D., Clark, A. D. Jr, Nanni, R. G., Ding, J., Jacobo-Molina, A., Kamer, G., Hughes, S. H., Arnold, E., Einspahr, H. M., Clancy, L. L., Rao, G. J., Cook, P. F., Harris, B. G., Munson, S. H., Finzel, B. C., McPherson, A., Weber, P. C., Lowandowski, F., Nagabhushan, T. L., Trotta, P. P., Reichert, P., Navia, M. A., Wilson, K. P., Thomson, J. A., Richards, R. R., Bowersox, K. D., Meade, C. J., Baker, E. S., Bishop, S. P., Dunbar, B. J. & Trinh, E. (1994). *J. Cryst. Growth*, **135**, 183–195.

Ducruix, A. & Giegé, R. (1999). Editors. *Crystallization of Nucleic Acids and Proteins. A Practical Approach.* Oxford: IRL Press.

Garcia-Ruiz, J. M. & Moreno, A. (1997). *J. Cryst. Growth*, **178**, 393–401.

Kuznetsov, Y. G., Malkin, A., Glantz, W. & McPherson, A. (1996). *J. Cryst. Growth*, **168**, 63–73.

Lee, J. C. & Lee, L. L. Y. (1981). *J. Biol. Chem.* **256**, 625–631.

Le Grimellec, C., Lesniewska, E., Giocondi, M. C., Finot, E., Vié, V. & Goudonnet, J. P. (1998). *Biophys. J.* **75**, 695–703.

Liu, X. Y., Boek, E. S., Briels, W. J. & Bennema, P. (1995). *Nature (London)*, **374**, 342–345.

Lorber, B., Sauter, C., Ng, J. D., Zhu, D. W., Giegé, R., Vidal, O., Robert, J. C. & Capelle, B. (1999). *J. Cryst. Growth*, **204**, 357–368.

Lorber, B., Sauter, C., Robert, J. C., Capelle, B. & Giegé, R. (1999). *Acta Cryst.* D**55**, 1491–1494.

McPherson, A. (1976). *J. Biol. Chem.* **251**, 6300–6303.

McPherson, A. (1998). *Crystallization of Biological Macromolecules.* Cold Spring Harbor, New York: Cold Spring Harbor Laboratory Press.

Malkin, A. J., Kuznetsov, Y. G. & McPherson, A. J. (1996). *J. Struct. Biol.* **117**, 124–137.

Malkin, A. J., Kuznetsov, Y. G. & McPherson, A. J. (1999). *J. Cryst. Growth*, **196**, 471–488.

Mikol, V. & Giegé, R. (1989). *J. Cryst. Growth*, **97**, 324–332.

Miller, T. Y., He, X. M. & Carter, D. C. (1992). *J. Cryst. Growth*, **122**, 306–309.

Moreno, A. & Soriano-Garcia, M. (1999). *Acta Cryst.* D**55**, 577–580.

Navaza, J. & Saludjian, P. (1997). *Methods Enzymol.* **276**, 581–594.

Ng, J. D., Kuznetsov, Y. G., Malkin, A., Keith, G., Giegé, R. & McPherson, A. (1997). *Nucleic Acids Res.* **25**, 2582–2588.

Ng, J. D., Lorber, B., Witz, J., Théobald-Dietrich, A., Kern, D. & Giegé, R. (1996). *J. Cryst. Growth*, **168**, 50–62.

Otwinowski, Z. & Minor, W. (1997). *Methods Enzymol.* **276**, 307–326.

Poterszman, A., Delarue, M., Thierry, J.-C. & Moras, D. (1994). *J. Mol. Biol.* **244**, 158–167.

Poterszman, A., Plateau, P., Moras, D., Blanquet, S., Mazauric, M. H., Kreuzer, R. & Kern, D. (1993). *FEBS Lett.* **325**, 183–186.

Riès-Kautt, M. M. & Ducruix, A. (1989). *J. Biol. Chem.* **264**, 745–748.

Robert, M. C., Bernard, Y. & Lefaucheux, F. (1994). *Acta Cryst.* D**50**, 496–503.

Sangwal, K. (1998). *Prog. Cryst. Growth Charact.* **36**, 163–248.

Sica, F., Demasi, D., Mazzarella, L., Zagari, A., Capasso, S., Pearl, L. H., D'Auria, S., Raia, C. A. & Rossi, M. (1994). *Acta Cryst.* D**50**, 508–511.

Timasheff, S. N. & Arakawa, T. (1988). *J. Cryst. Growth*, **90**, 39–46.

Vidal, O., Robert, M. C., Arnoux, B. & Capelle, B. (1999). *J. Cryst. Growth*, **196**, 559–571.

Vidal, O., Robert, M. C. & Boué, F. (1998). *J. Cryst. Growth*, **192**, 257–270.

Zhu, D. W., Han, Q., Qiu, W., Campbell, R. L., Xie, B. X., Azzi, A. & Lin, S.-X. (1999). *J. Cryst. Growth*, **196**, 356–364.